Available online at www.sciencedirect.com
ScienceDirect
Journal of Power Sources 159 (2006) 1283–1290
JOURNAL OF POWER SOURCES
www.elsevier.com/locate/jpowsour

Autothermal reforming study of diesel for fuel cell application

Inyong Kang, Joongmyeon Bae *

Department of Mechanical Engineering, Korea Advanced Institute of Science and Technology (KAIST), Daejeon, South Korea

Received 6 October 2005; received in revised form 17 December 2005; accepted 20 December 2005
Available online 8 February 2006

Abstract

Diesel is one of the best hydrogen storage systems, because of its very high hydrogen volumetric density (100 kg H_2 m^{-2}) and gravimetric density (15% H_2). In this study, several catalysts were selected for diesel reforming. Three experimental catalysts (Pt on gadolinium-doped ceria, Rh and Ru on the same support) and two commercial catalysts (FCR-HC14 and FCR-HC35, Süd-Chemie, Inc.) were used to reform diesel. The effects of operating conditions, such as temperature, O_2/C16 and H_2O/C16 on autothermal reforming (ATR) were investigated. In addition, by analyzing the concentrations of products and the temperature profiles along the catalyst bed, we studied the reaction characteristics for a better understanding of the ATR reaction. The fuel delivery and heat transfer between the front exothermic part and the rear endothermic part of the catalyst bed were found to be significant. In this study, the characteristic differences between a surrogate fuel ($C_{16}H_{34}$) and commercial grade diesel for the ATR were also examined.

Keywords: Fuel cell; Hydrogen; Autothermal reforming; Hexadecane; Diesel

1. Introduction

It is believed that fuel cells will be one of the main energy conversion systems of the future. Fuel cells have higher energy conversion efficiencies and lower amounts of emission gases than internal combustion engines. Hydrogen can be converted at a very high electrochemical efficiency and emits only water as a by-product. However, there is, at present, lack of a hydrogen production infrastructure. There are two main ways to produce hydrogen: one is by the electrolysis of water, the other is by reforming of fossil fuels, such as natural gas, gasoline and diesel. It has been suggested that fuel reforming is the more practical method due to its high-energy efficiency. In this study, diesel was chosen as a fuel, because of its high gravimetric and volumetric hydrogen density and a well-established delivery infrastructure. In spite of these advantages of diesel, diesel reforming is not preferred because there are several problems such as a high coking probability [1–5], sulfur poisoning [2,3,6–8], an inefficient mixing of diesel with other reactants [8] and hydrocarbon breakthroughs [6,8] at high gas flows. This study deals with the basic reforming characteristics, such as the effects of the operating conditions and the temperature profiles, in catalyst bed.

Three mechanisms can be used to reform hydrocarbons [1,6,9–11]: steam reforming (SR), partial oxidation (POX) and autothermal reforming (ATR). These three mechanisms are represented by the following chemical reactions, using an assumption of CO_2 formation for all the carbon involved. (Hexadecane ($C_{16}H_{34}$) was used as a surrogate of diesel.)

$$\text{SR}: \quad C_{16}H_{34} + 32H_2O \rightarrow 49H_2 + 16CO_2; \quad \Delta H = 2336\,\text{kJ}$$

$$\text{POX}: \quad C_{16}H_{34} + 16O_2 \rightarrow 17H_2 + 16CO_2; \quad \Delta H = -5694\,\text{kJ}$$

$$\text{ATR}: \quad C_{16}H_{34} + 16H_2O + 8O_2 \rightarrow 33H_2 + 16CO_2; \quad \Delta H = -1739\,\text{kJ}$$

Using steam reforming to produce hydrogen with fuel and water is a very mature technology used to make syngas ($H_2 + CO$) in the chemical industry. Steam reforming has several advantages, such as a high hydrogen concentration (over 70% on a dry basis) and long-term stability at a steady state. However, SR requires a high volume reactor due to its characteristically intense endothermic reaction. One of the main technical issues for a SR reactor is not kinetics but heat transfer. An SR reactor should be designed with the desired heat transfer. It is difficult

* Corresponding author. Tel.: +82 42 869 5045; fax: +82 42 869 3217.
E-mail address: jmbae@kaist.ac.kr (J. Bae).

0378-7753/$ – see front matter © 2006 Elsevier B.V. All rights reserved.
doi:10.1016/j.jpowsour.2005.12.048

to start a SR reactor quickly, and the reactor has a slow system response. Consequently, it is appropriate only for large-scale plants.

Unlike typical combustion, the POX mechanism uses fuel and oxygen to produce hydrogen by utilizing lower stoichiometric oxygen. It is easy to start a POX reactor quickly due to the high exothermicity of POX. Therefore, it is appropriate for small systems. However, the concentration of the hydrogen produced using POX is lower than that of using SR. In addition, the high temperatures associated with the POX process create difficulties with regard to materials selection. Moreover, the high possibility of coke formation is another disadvantage of using POX.

The ATR mechanism involves a combination of the two aforementioned reactions. The total heat balance in an ATR can be controlled by changing the degree of the exothermic and endothermic reactions. Thus, the ATR requires no external heat source unlike SR and the reaction temperature can be kept lower than that of POX. The advantages of ATR make possible simple and small reactors with relatively high efficiency. Furthermore, the presence of water with oxygen to reform diesel makes the probability of coke formation low. Oxygen facilitates a fast ATR reaction. The concentration of hydrogen produced by the ATR reaction is higher than that of POX.

Nevertheless, an ATR mechanism is not straightforward, and it requires sophisticated operating techniques for a proper combination of the POX and SR [12]. In this study, we used the ATR mechanism to reform diesel fuel. This study was concerned with the effects of operating conditions on ATR reaction and with the analysis of reaction characteristics in the catalyst bed.

2. Thermodynamics of ATR for diesel

The product gas compositions of ATR for diesel can be thermodynamically calculated as functions of temperature based on the principle of Gibbs free energy minimization. Hexadecane ($C_{16}H_{34}$) was used as a surrogate of diesel for the thermodynamic estimation.

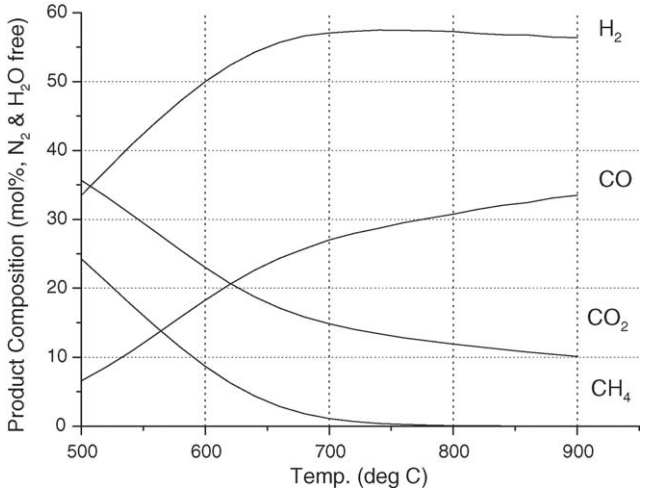

Fig. 1. Thermodynamic equilibrium compositions ($C_{16}H_{34}$, $O_2/C = 0.5$, $H_2O/C = 1.25$).

Fig. 1 shows that the highest concentration of hydrogen can be obtained at about 750 °C. At that temperature, the concentrations of H_2, CO and CO_2 are 57%, 29% and 13%, respectively. The H_2 and CO increase steadily until 700 °C, and then the H_2 line flattens; however, the CO continues to increase, even at temperatures higher than 700 °C.

A generic ATR reaction for hydrocarbon can be expressed as follows [9]. (It is assumed that products contain only H_2 and CO_2.)

$$C_nH_mO_p + x(O_2 + 3.76N_2) + (2n - 2x - p)H_2O = nCO_2 + \left(2n - 2x - p + \frac{m}{2}\right)H_2 + 3.76xN_2$$

(x : O_2 to fuel molar ratio) [9] (1)

In Eq. (1), the required amount of reactant water changes depending on the amount of O_2. As "x" decreases, more H_2O is required. If x is 0, ATR is equal to SR. For Eq. (1) the heat of the reaction can be described by Eq. (2), in which ΔH_r represents the heat of the reaction, as follows:

$$\Delta H_r = n\,\Delta H_{f,CO_2} - (2n - 2x - p)\Delta H_{f,H_2O} - \Delta H_{f,fuel} \quad [9] \tag{2}$$

If $C_{16}H_{34}$ is applied as a fuel, then ΔH_r at 298 K can be calculated as follows:

$$\Delta H_{r,298} = 16(-94051) - (32 - 2x)(-68318) - (-108871) = 790231 - 136636x \quad (0 \le x \le 16)$$

(if $x = x_0 = 5.78$, $\Delta H_r = 0$)

In the above equation, x represents a value between 0 and 16. When x becomes larger, the exothermicity becomes higher. For a case in which x is larger than 16, water is produced. When x is 5.78 ($x = x_0$), the heat of reaction becomes 0. The efficiency of a fuel reformer can be defined as follows:

$$\text{Efficiency (\%)} = \frac{\text{Lower heating value of hydrogen produced}}{\text{Lower heating value of fuel used}} \tag{3}$$

In Eq. (3), the numerator is expressed as the product of the hydrogen yield × the heat of combustion of hydrogen, that is

$$= \left[2n - 2x - p + \left(\frac{m}{2}\right)\right] 57.797\ \text{cal/mol of}\ C_nH_mO_p \quad [9]$$

In the range of $x \ge x_0$ (=5.78), the LHV of fuel used is equal to the combustion heat. However, in the endothermic range of $x < x_0$, additional heat is needed for the reaction. Therefore, in the denominator of Eq. (3), the fuels used comprise the fuel to be reformed and any additional fuel needed to supply heat for an endothermic reaction.

Fig. 2 shows the thermal efficiency of the fuel reformer in accordance with Eq. (3). As x increases, H_2 decreases linearly. In the endothermic region of $x < x_0$, additional heat for an endothermic reaction is required. However, in the exothermic range of $x \ge x_0$, the LHV of fuel is parallel to the x-axis, because there is no demand for additional heat. Efficiency reaches a maximum of 91% at $x = 5.78$. For practical purposes, however, it is

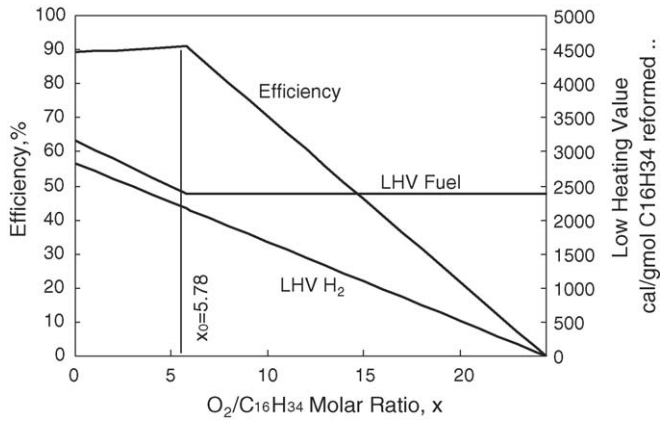

Fig. 2. Thermal efficiency (from [1]).

better to make ATR a slightly exothermic reaction to enable a self-sustaining operation. It is, therefore, appropriate that a final O_2/C16 have a value larger than x_0 (=5.78) [10].

The stoichiometry of H_2O (=20.44) is calculated simply using Eq. (1) for $x_0 = 5.78$. However, when the amount of water to supply is being determined, the possibility of coke formation has to be considered [6]. We have to calculate a minimum value of H_2O/C16 that will inhibit coke formation. Fig. 3 shows the free range of H_2O/C16 for coke formation under the condition of a fixed O_2/C16. As the value of H_2O/C16 ratio increase, the minimum temperature necessary to inhibit the coke formation decreases. For an experiment at about 700 °C, the required value of H_2O/C16 necessary to inhibit coke formation is approximately 5 as seen in Fig. 3.

3. Experimental

3.1. Experimental setup

Hexadecane (Sigma–Aldrich, 99%) and commercial diesel (LG–Caltex Oil) were used as fuels. Air and vaporized steam were added with fuel into a reactor. Fuel and water were injected using an HPLC pump (MOLEH Co., Ltd.), while air was injected and controlled using a mass flow controller (MKS). Ultra Pure (15 MΩ) water was used. An external heat exchanger to vaporize

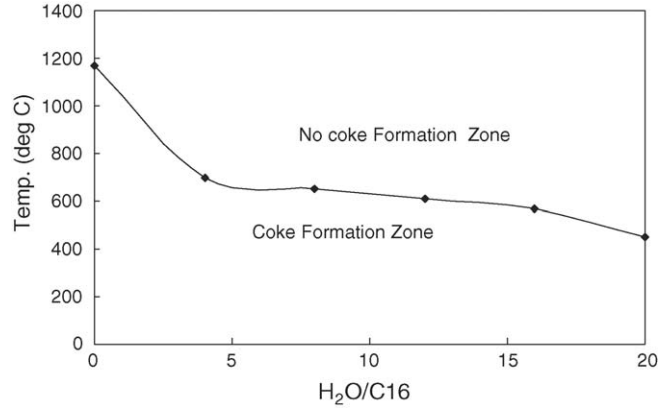

Fig. 3. H_2O/C effect on coke formation ($C_{16}H_{34}$, O_2/C16 = 8).

water was installed and the vaporized water was carried by N_2. The reactor temperature was controlled with an electric furnace. Product gases were analyzed with a GC-MS (Agilent 6890N) after a moisture removal procedure. Fig. 4 illustrates the experimental setup schematically.

3.2. Reactor

Two k-type thermocouples were installed at the top and the bottom of the catalyst bed. Three noble metal catalysts (Pt, Rh, Ru) on doped CeO_2 were selected to reform diesel using a patented method for catalyst formulation from the Argonne National Laboratory, U.S.A. (abbreviated as NECS-1, NECS-2 and NECS-3, respectively) [13,14]. Fine powders of the catalysts were prepared using a combustion method. After the catalysts were pressed to pellet size, they were crushed into granules with regular size (250–710 μm). To estimate the performance of our catalysts, we compared them with commercial catalysts (FCR-HC14 and FCR-HC35, Süd-Chemie).

3.3. Experimental results and discussion

3.3.1. Effects of catalysts, temperature, O_2/C16 (oxygen/carbons ratio) and H_2O/C16 (steam/carbon ratio)

Figs. 5 and 6 show the experimental results of the ATR reactions of $C_{16}H_{34}$ with the three experimental catalysts (NECS-1, NECS-2 and NECS-3) and the two commercial catalysts (FCR-HC14 and FCR-HC35). In the experiment, the O_2/C16, H_2O/C16 and gas hourly space velocity (GHSV) were 8, 20 and 5000 h^{-1}, respectively [12]. Fuel conversion percentage was determined using the following equation [15]:

$$\text{Fuel conversion}\,(\%) = \frac{\text{Fuel reacted}}{\text{Fuel used}} \times 100 \quad (4)$$

Theoretically, the fuel conversion is determined using Eq. (4). In this study, however, the fuel conversion was determined using Eq. (5), due to several practical reasons, such as limitation of gas analysis and the removal of liquid hydrocarbon during the water condensation process.

$$\text{Fuel conversion}\,(\%) = \frac{\text{The total number of carbonin CO, CO}_2\text{ and CH}_4\text{ in product}}{\text{Carbon number in fuel used}} \times 100 \quad (5)$$

Fig. 5 shows that the thermodynamic maximum concentration of hydrogen in the product reaches 57% at 800 °C. The H_2 of NECS-1, NECS-2, NECS-3, FCR-HC14 and FCR-HC35 are 56%, 55%, 49%, 52% and 56% at 800 °C, respectively.

The absolute concentration ratios of respective products for 1 mol feed of $C_{16}H_{34}$ are presented in Fig. 6. The figure illustrates that NECS-1 is superior to the other catalysts. Therefore, NECS-1 was chosen as the catalyst used for further study. After selecting a catalyst, the effects of temperature, oxygen to carbon ratio (O_2/C16) and steam to carbon ratio (H_2O/C16) on product compositions and fuel conversions were investigated.

The effect of temperature on the product composition is shown in Fig. 7. As the temperature increases, H_2 and CO

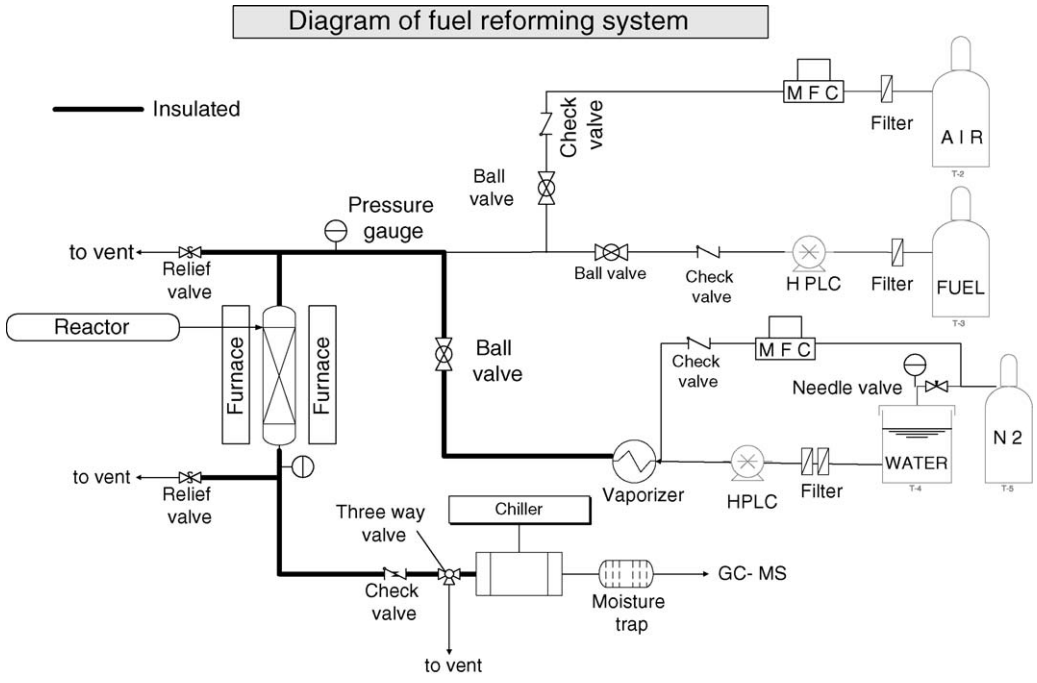

Fig. 4. Schematic experiment design.

simultaneously increase. At 850 °C, the composition of H_2 is maximized. This is a higher temperature than the thermodynamically calculated 750 °C to maximize H_2 production. Poor fuel conversion was observed at temperatures lower than 750 °C, as seen in Fig. 7. We investigated the effects of O_2/C16 and H_2O/C16 on the product compositions in more detail at 850 °C, where the maximum of H_2 was obtained. Figs. 8 and 9 show the effects O_2/C16 and H_2O/C16, respectively.

The concentrations of H_2 and CO decreased at higher O_2/C16 ratio due to oxidation. In addition, the O_2/C16 ratio greatly affects the reactor temperature due to higher exothermicity and subsequently fuel conversion [6], coke formation and self-sustenance of a reactor.

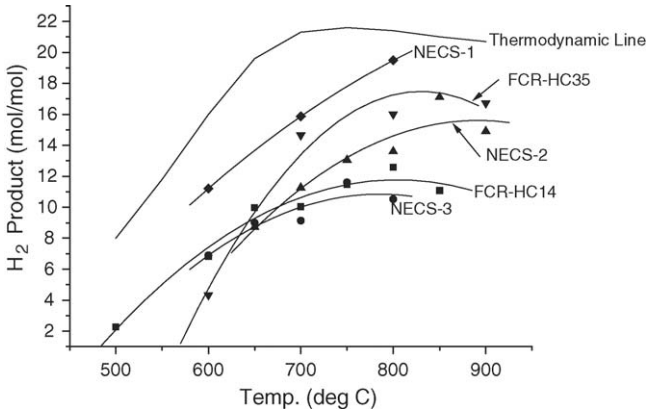

Fig. 6. Comparison of ATR catalysts at various temperatures:H_2 production (mol mol^{-1} $C_{16}H_{34}$) ($C_{16}H_{34}$ = 0.028 ml min^{-1}, O_2/C16 = 8, H_2O/C16 = 20, GHSV = 5000 h^{-1}).

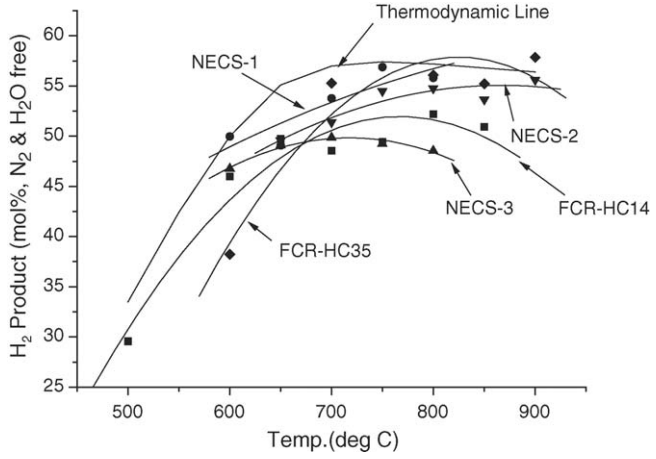

Fig. 5. Comparison of ATR catalysts at various temperatures: H_2 production (mol%, N_2 and H_2O free) ($C_{16}H_{34}$ = 0.028 ml min^{-1}, O_2/C16 = 8, H_2O/C16 = 20, GHSV = 5000 h^{-1}).

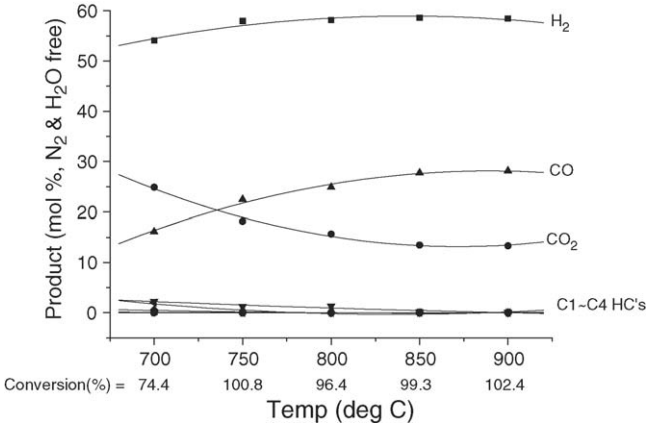

Fig. 7. Compositions of product gases as a function of temperature ($C_{16}H_{34}$ = 0.057 ml min^{-1}, O_2/C16 = 12, H_2O/C16 = 20, NECS-1, GHSV = 5000 h).

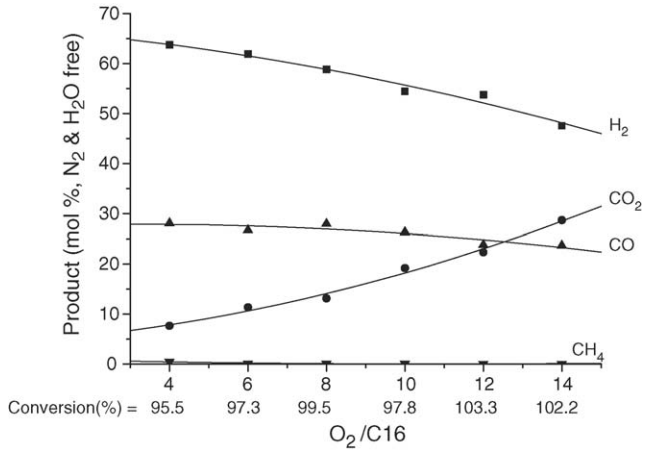

Fig. 8. O_2/C16 effect on product gases for the $C_{16}H_{34}$ ATR reaction ($C_{16}H_{34}$ = 0.057 ml min^{-1}, H_2O/C16 = 20, 850 °C, NECS-1, GHSV = 5000 at O_2/C16 = 12).

Therefore, a proper value of O_2/C16 has to be determined by considering not only the H_2 concentration but also other factors, such as fuel conversion and coke formation. For thermal efficiency O_2/C16 = 5.78 (at the heat of reaction, $\Delta H_r = 0$) would be preferable. However, a higher value of O_2/C16 than 5.78 is necessary for practical reasons, such as the self-sustenance of a reactor [8].

Fig. 9 shows the H_2O/C16 effects on the ATR reaction at a fixed O_2/C16 ratio. As H_2O/C16 ratio increases, the concentrations of H_2 and CO_2 increase, while that of CO decreases. These results were caused by the water gas shift (WGS) reaction of CO oxidation by H_2O.

$$CO + H_2O \rightarrow H_2 + CO_2: \quad \text{water gas shift reaction}$$

When H_2O/C16 ratio increases, it can be predicted that H_2 production will increase and that the temperature of the catalyst bed will decrease due to the endothermicity of the SR reaction [10]. However, this phenomenon was not observed in the experiment. The measured temperatures of the catalyst bed were nearly

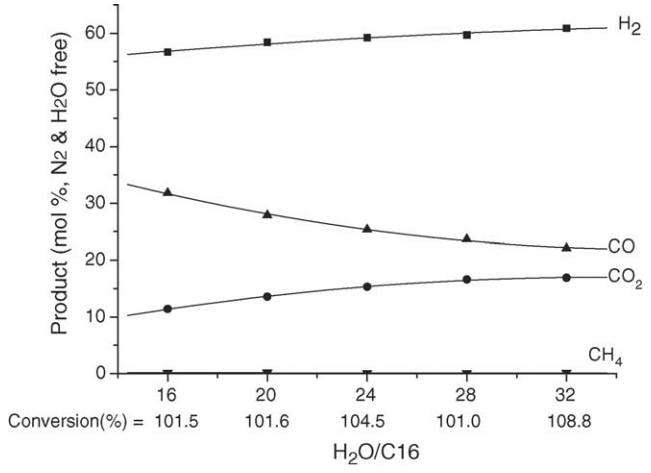

Fig. 9. H_2O/C16 effect on product gases for the $C_{16}H_{34}$ ATR reaction ($C_{16}H_{34}$ = 0.057 ml min^{-1}, O_2/C16 = 12, 850 °C, NECS-1, GHSV = 5000 h^{-1} at H_2O/C16 = 20).

unchanged for different H_2O/C16 ratios. A H_2O/C16 ratio of 16 is sufficient to reform diesel. When a higher H_2O/C16 ratio is applied, the extra water does not participate in the SR reaction but participate in the WGS reaction. To confirm this, the concentrations of H_2 and CO_2 after the WGS reaction were estimated for H_2O/C16 = 16 and 28 as presented below.

When product gases are:

$$xH_2 + yCO + zCO_2 + wH_2O \tag{6}$$

and the CO is reduced by as much as Δy by the WGS reaction, then the following reaction may occur:

$$\Delta yCO + \Delta yH_2O \rightarrow yH_2 + \Delta yCO_2 \tag{7}$$

(It is assumed that enough H_2O is supplied to enable a WGS reaction.)

From (6) and (7)

$$(x + \Delta y)H_2 + (y - \Delta y)CO + (z + \Delta y)CO_2 + (w - \Delta y)H_2O$$

(on the dry basis, $x + y + z = 100$)

After a WGS reaction, H_2 concentration in the product is described as follows:

$$= \frac{x + \Delta y}{(x + \Delta y) + (y - \Delta y) + (z + \Delta y)} = \frac{x + \Delta y}{x + y + z + \Delta y}$$

$$= \frac{x + \Delta y}{100 + \Delta y} \tag{8}$$

The CO_2 concentration can be written in manner similar to that of H_2

$$= \frac{z + \Delta y}{100 + \Delta y} \tag{9}$$

The experimental results show that x, y and z are 56.7, 31.8 and 11.4, respectively, at H_2O/C16 = 16. The CO is reduced by as much as 8.2 when the H_2O/C16 ratio changes from 16 to 28 (therefore, $\Delta y = 8.2$). From (8) and (9):

$$H_2 \text{ after WGS reaction} = \frac{56.7 + 8.2}{100 + 8.2} = 59.98$$

$$CO_2 \text{ after WGS reaction} = \frac{11.4 + 8.2}{100 + 8.2} = 18.1$$

The calculated values of H_2 and CO_2 are in good agreement with the experimental data as summarized in Table 1.

Consequently, it is reasonable to consider that the WGS occurs when additional water is provided. The proper range of H_2O/C16 ratio for an ATR reaction can be determined in accordance with several considerations such as product composition, thermodynamic coke formation zone. A minimum value has to

Table 1
Product comparison (mol%)

H_2O/C16	H_2	CO	CO_2
16 (Experiment)	56.7	31.8	11.4
28 (Experiment)	59.7	23.6	16.6
28 (Calculated)	59.98	23.6	18.11

be determined to inhibit coke formation. In Fig. 3, we already know that thermodynamically, a value of H_2O/C16 needs about 5 at 700 °C. To determine the maximum value of H_2O/C16, we need to calculate the amount of stoichiometric water necessary to reform fuel into H_2 and CO_2 at a fixed O_2/C. If we use more water than stoichiometric demand, then additional water is utilized in the WGS reaction as in the aforementioned experiment. According to Eq. (1), an H_2O/C16 value for which $C_{16}H_{34}$ is totally converted to H_2 and CO_2 can be determined with a given O_2/C16 (=8, determined experimentally). Therefore, in terms of stoichiometry for an ATR reaction, H_2O/C16 = 16 is sufficient. However, a higher amount of H_2O was selected in this study for pragmatic reasons, such as the suppression of coke formation. In future studies, we are going to investigate the relationship of H_2O/C16 ratio and coke formation experimentally. Ultimately, we chose H_2O/C16 = 20, which is slightly higher than the stoichiometric demand at O_2/C16 = 8. It should be noted that a larger water supply also requires more heat to evaporate the water to steam, and this should be considered during system design [8,10].

We investigated the concentration and temperature profiles along the catalyst bed for a better understanding of an ATR reaction. The upper chart in Fig. 10 shows the product concentrations (mol mol^{-1} $C_{16}H_{34}$) along the length of the catalyst bed. The length of the catalyst bed increased with increasing catalyst loading to the reactor as it is very obvious. To remove the degradation effect of the catalyst, fresh catalysts were continuously loaded to the reactor. Product gas compositions and temperature at the top and the bottom of the reactor were also monitored. A different experimental setup was prepared to monitor the temperature profile at the reactor by using multiple thermocouples in a long catalyst bed (=2 in. long)

The middle chart in Fig. 10 shows the temperatures monitored in the catalyst bed using multiple thermocouples. A reactor was operated at 850 °C using an electric furnace, with O_2/C16 = 12 and H_2O/C16 = 20. A constant flow of N_2 was supplied to evaluate effect of furnace on temperature profile. The lower part of Fig. 10 provides a schematic of the experimental setup (the actual reactor setup had a vertical configuration). The first point at $x = 0.25$ in. is just before the catalyst bed. This is a non-catalytic zone, where the thermal cracking of hydrocarbons, POX and total combustion may occur, as described below [1,2].

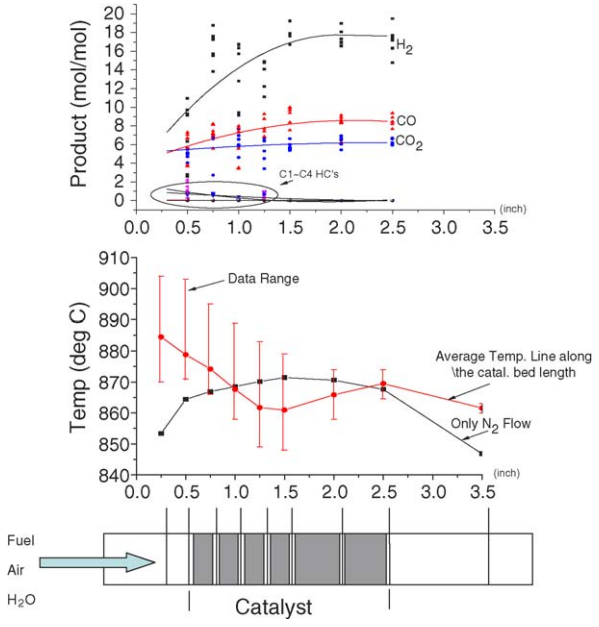

Fig. 10. Concentration and temperature profiles along the catalyst bed ($C_{16}H_{34}$ = 0.0567 ml min^{-1}, O_2/C16 = 12, H_2O/C16 = 20).

Thermal cracking : $C_{16}H_{34} \rightarrow CH_4,\ C_2H_6,\ C_2H_4,\ C_3H_8,\ C_4H_{10},\ C_5H_{12},\ C_6H_{12}$ (cyclohexane), C_6H_6 (benzene) and C_8H_{18} (isooctane)

$$\text{POX}: \quad C_nH_m + nO_2 = \frac{m}{2}H_2 + nCO_2$$

$$C_nH_m + \frac{n}{2}O_2 = \frac{m}{2}H_2 + nCO$$

$$\text{Total combustion}: \quad C_nH_m + \left(\frac{m}{4} + n\right)O_2 = \frac{m}{2}H_2O + nCO_2$$

The analysis result shows that unreacted hydrocarbons are present until $x = 1.25$ and diminish negligibly from the position $x = 1.5$ as seen in Fig. 10. The H_2 and CO compositions are also in good agreement with existence of hydrocarbons and saturates from the position $x = 1.5$. Both the product gas compositions and temperature profiles show a relatively large error bar of data point. Those are considered to be due to the non-uniform delivery problem of the fuel. The $C_{16}H_{34}$, with a boiling point of 287 °C, is difficult to vaporize. In addition, the fuel-transfer pump usually pulsates at a low flow rate. Even though the average flow rate remains constant, a momentary flow rate pulsates continuously. Moreover, liquid fuel is injected directly into the reactor. So the fuel is difficult to mix H_2O and O_2 for the short time. These reasons would create serious variation of temperature and concentrations. This fuel delivery problem will have to be solved to construct efficient ATR reactor for diesel.

Through the temperature profile measurement, it was clearly shown that the ATR reactor comprises a severe exothermic reaction at the front of catalyst bed followed by an intense endothermic reaction. As mentioned in the above thermodynamic discussions, ATR is a combination of POX and SR. In actuality, however, the two reactions do not seem to occur simultaneously due to different rate of reaction [6,8,10,16]. The major portion of H_2 is produced from the endothermic reaction, SR zone. The SR is activated by the heat from the POX and an electric furnace. For practical design consideration, a furnace has to be replaced as insulator. Consequently, only the thermal energy from the POX would activate the SR, with no external heat source. The heat transfer between the POX and the SR zones will be a key engineering issue as well as the fuel delivery problem.

The rear part of catalyst bed has smaller temperature variations than that of the front part. Especially the H_2 composition starts to be saturated from $x = 1.5$, where the concentration of H_2 is 55%, which is a similar value to that obtained during screening process of the catalysts.

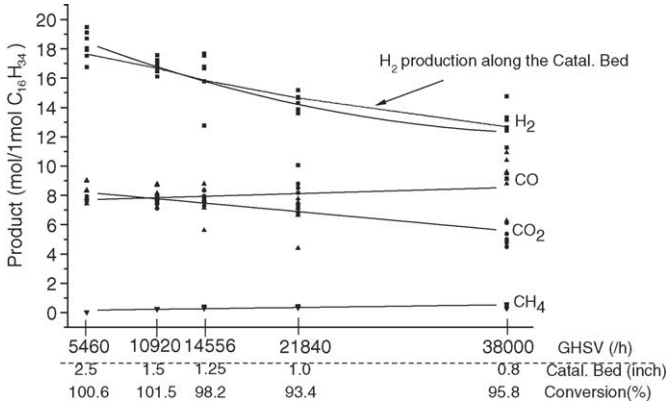

Fig. 11. GHSV effect on product gases for the $C_{16}H_{34}$ ATR reaction ($C_{16}H_{34}$ = 0.057–0.418 ml min^{-1}, H_2O/C16 = 20, O_2/C16 = 12, 850 °C).

The resultant product gas composition for various positions of the reactor was confirmed using another experimental setup, which changes gas hourly space velocity (GHSV) (h^{-1}) by changing the reactant flow rate and monitors product gas compositions as seen in Fig. 11. The two independently determined experimental results showed reasonably good agreement.

3.3.2. ATR of commercial diesel

Fig. 12 shows the results of the surrogate $C_{16}H_{34}$ and commercial diesel reforming under the same conditions. The H_2O/C16 ratio and O_2/C16 ratio are 20 and 8, respectively. The H_2 concentration of the commercial diesel is much lower than that of the surrogate. For the surrogate, the H_2 concentration was maximized at 750 °C; in contrast, the H_2 concentration of diesel reached a maximum at 800 °C. The maximum concentration of H_2 in the surrogate and the diesel are 59% and 53%, respectively. Unreacted hydrocarbons of the surrogate nearly diminished from 750 °C. However, the product of commercial diesel contains an average of 3.2% CH_4 for all ranges of temperatures. As a result, the ATR performance of diesel is inferior to the surrogate $C_{16}H_{34}$.

Generally diesel comprises numerous components. Particularly, non-paraffins in diesel, such as aromatics, seem to make it difficult to reform diesel. The effects of components on diesel

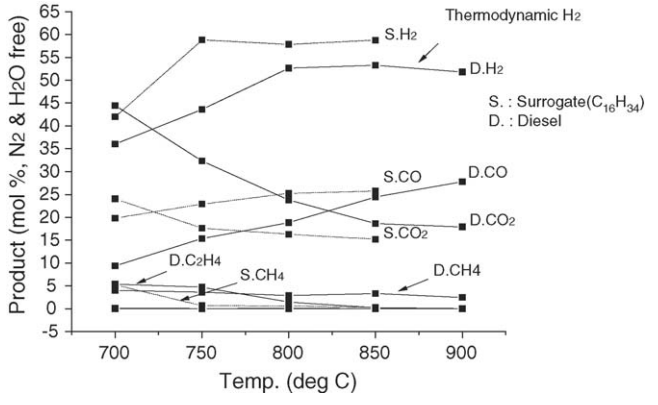

Fig. 12. ATR reaction results of $C_{16}H_{34}$ and diesel at various temperatures (fuel = 0.068 ml min^{-1}, H_2O = 0.084 ml min^{-1}, air = 217 ml min^{-1}, NECS-1).

ATR reaction are currently being studied and will be reported in the near future.

4. Conclusion

A Pt catalyst on doped cerium oxide showed excellent performance compared to the other catalysts in our study. In the case of surrogate $C_{16}H_{34}$, the concentration of H_2 was maximized at 800 °C. Fuel conversion was nearly 100% at temperatures higher than 750 °C. In terms of thermal efficiency, O_2/C16 = 5.78 showed the best result; however, in an actual application, O_2/C16 values of slightly higher than 5.78 should be used for self-sustenance of an ATR reactor. If H_2O/C16 values of higher than 16 are used with a fixed O_2/C16 (=8), the additional H_2O does not participate in the SR reaction but participates in the WGS reaction.

Both the product gas compositions and temperature profiles along the catalyst bed showed a relatively large error bar of data point due to a non-uniform fuel delivery problem. Using the temperature profile, it was clearly shown that an ATR reactor comprises a severe exothermic reaction at the front of catalyst bed and a subsequent intense endothermic reaction in the rear of catalyst bed due to different kinetics in POX and SR. The major portion of H_2 is produced from the endothermic reaction, the SR zone. Thermal energy from the POX leads the SR with no external heat source. Heat transfer between the POX and the SR zone will be a key engineering issue as well as fuel delivery.

It was more difficult to reform diesel than surrogate $C_{16}H_{34}$. This seems to be due to non-paraffins in diesel. The effects of fuels on ATR will be reported in the future.

Acknowledgments

This work has been funded by the Korea Institute of Science and Technology (KIST) and the Korea Institute of Industrial Technology Evaluation and Planning (ITEP). Analysis facilities, such as the GC-MS and the SEM/EDX have been supported by the Ministry of Education and Human Resources Development.

References

[1] S. Ayabe, H. Omoto, T. Utaka, R. Kikuchi, K. Sasaki, Y. Teraoka, K. Eguchi, Catalytic autothermal reforming of methane and propane over supported metal catalysts, Appl. Catal. A: Gen. 241 (2003) 261–269.
[2] P.K. Cheekatamarla, W.J. Thomson, Poisoning effect of thiophene on the catalytic activity of molybdenum carbide during tri-methyl pentane reforming for hydrogen generation, Appl. Catal. A: Gen. 287 (2005) 176–182.
[3] P.K. Cheekatamarla, A.M. Lane, Catalytic autothermal reforming of diesel fuel for hydrogen generation in fuel cells. II. Catalyst poisoning and characterization studies. J. Power Sources (2005), in press.
[4] Y. Sone, H. Kishida, M. Kobayashi, T. Watanabe, A study of carbon deposition on fuel cell power plants—morphology of deposited carbon and catalytic metal in carbon deposition reactions on stainless steel, J. Power Sources 86 (2000) 334–339.
[5] A. Shamsi, J.P. Baltrus, J.J. Spivey, Characterization of coke deposited on Pt/alumina catalyst during reforming of liquid hydrocarbons, Appl. Catal. 293 (2005) 145–152.
[6] P.K. Cheekatamarla, A.M. Lane, Catalytic autothermal reforming of diesel fuel for hydrogen generation in fuel cells. I. Activ-

ity tests and sulfur poisoning, J. Power Sources 152 (2005) 256–263.
[7] X. Ma, L. Sun, C. Song, A new approach to deep desulfuriztion of gasoline, diesel fuel and jet fuel by selective adsorption for ultra-clean fuels and for fuel cell applications, Catal. Today 77 (2002) 107–116.
[8] B. Lenz, T. Aicher, Catalytic autothermal reforming of jet fuel, J. Power Sources 149 (2005) 44–52.
[9] S. Ahmed, M. Krumpelt, Hydrogen from hydrocarbon fuels for fuel cells, Int. J. Hydrogen Energy 26 (2001) 191–301.
[10] S.H.D. Lee, D.V. Applegate, S. Ahmed, S.G. Calderone, T.L. Harvey, Hydrogen from natural gas: part I - autothermal reforming in an integrated fuel processor, Int. J. Hydrogen Energy 30 (2005) 829–842.
[11] A. Qi, S. Wang, G. Fu, D. Wu, Autothermal reforming of *n*-octane on Ru-based catalysts, App. Catal. A: Gen. 293 (2005) 71–82.
[12] C. Pereira, J.-M. Bae, S. Ahmed, M. Krumpelt, Liquid fuel reformer development: autothermal reforming of diesel fuel, Argonne National Laboratory Chemical Technology Division, Argonne, IL 60439, USA, 2001.
[13] M. Krumpelt, R. Wilkenhoener, D.J. Carter, J.-M. Bae, J.P. Kopasz, T. Krause, S. Ahmed, Catalytic autothermal reforming, Annual Progress Report, U.S. Department of Energy, 2000, pp. 65–70.
[14] M. Krumpelt, T. Krause, J.D. Carter, J. Mawdsley, J.-M. Bae, S. Ahmed, C. Rossignol, Catalytic autothermal reforming, Annual Progress Report, U.S. Department of Energy, 2001, pp. 99–95.
[15] R.W. Misson, C.A. Mims, B.A. Saville, Introduction to chemical reaction engineering and kinetics, CH. 5.2, Department of Chemical Engineering and Applied Chemistry, University of Toronto, USA, 1999.
[16] A. Heinzel, B. Vogel, P. Hübner, Reforming of natural gas-hydrogen generation for small scale stationary fuel cell systems, J. Power Sources 105 (2002) 202–207.